UNSUPERVISED CLASS-EXPERT LEARNING FOR SUPPORTING COVID-19 TRIAGE BASED ON COMPUTED TOMOGRAPHY DATA

Taís Aparecida Alvarenga , Luís Otávio Santos
Postgraduate Program in Systems Engineering and Automation, Federal University of Lavras.
{tais.alvarenga, luis.santos3}@estudante.ufla.br

Demóstenes Zegarra Rodríguez
Department of Computer Science, Federal University of Lavras
{demostenes.zegarra}@ufla.br

Danton Diego Ferreira , Bruno Henrique Groenner Barbosa
Department of Automatic, Federal University of Lavras
{danton, brunohb}@ufla.br

Jose Manoel de Seixas
Signal Processing Laboratory, COPPE/POLI, Federal University of Rio of Janeiro
{seixas}@lps.ufrj.br

Abstract – Deep learning applications in medical imaging have been achieving promising results in the detection of diseases, among which clinical trials in terms of screening and diagnosis of patients with COVID-19 stand out. Computed Tomography (CT) images of the chest have been used by specialists for the diagnosis of COVID-19. However, due to the need of the moment and the possibility of using computational resources to help the medical team, it is observed in the literature several proposed works using supervised learning, however it lacks unsupervised methods for the screening and diagnosis of patients with COVID-19. In this work, the deep learning models *Convolutional Neural Network* (CNN) and Variational Autoencoders are used for feature extraction and later this information is used for binary and multiclass classification in unsupervised methods (k-means, Fuzzy C-Means and Self-Organizing Maps). For this purpose, a public database containing 4173 CT images (2168 CT slices from COVID-19, 758 slices from Healthy and 1247 slices from other lung diseases) was used. The results show that feature extraction via Variational Autoencoders has similar performance with state-of-the-art models in the literature for COVID-19, mainly for the binary classification with accuracies of 95.9%, 92.1% and 95.9% for k-means, Fuzzy C-Means and SOM, respectively, presenting competitive results in the literature. It also shows the importance of extracting features through convolutional networks to improve classification performance, resulting from the use of deep learning and its state of the art in the area of computer vision.

Keywords – COVID-19, Unsupervised Learning, Transfer Learning, Variational Autoencoder, *k-means, Fuzzy C-Means*

1 Introduction

COVID-19 is an infectious disease caused by the etiologic agent, Severe Acute Respiratory Syndrome, Coronavirus 2(SARS-CoV-2) [1], which has had a high mortality rate compared to other influenzas [2]. By February 2022, more than

5.6 million deaths had been recorded, surpassing morbidities such as SARS-CoV and MERS-CoV [3]. In mid-2019,with the emergence of COVID-19 in the city of Wuhan (China) [4], the use of computational intelligence techniques became an essential tool in supporting the decision-making of doctors and/or specialists [5, 6]. Given the ease of spread and contagion, measures such as social isolation have been imposed in many countries, which makes the use of various technological resources to control this disease even more significant.

Currently, the diagnosis of the disease is performed through Reverse Transcription Polymerase Chain Reaction (RT-PCR), clinical history of the patient and medical images, such as computed tomography (CT) images. AlthoughCT images play an important role in the diagnosis of COVID-19, this method has some limitations such as the lack of specificity between the lesions that may have been caused by other diseases, as well as the lack of professionals forthe evaluation. In this context, the use of computational tools may overcome these issues [7].

On the other hand, the increase of available data (big data) boosted the development and improvement of *Deep Learning* technique [8], such as convolutional neural networks [9]: *ResNet* [10], Efficient Network [11], among other models that have shown expressive results, mainly for feature extraction, a crucial step to improve the classification rates. These models have shown good results in several areas [12], especially for screening and diagnosis of COVID-19 based on CT [13]. The works reported in [14,15] have demonstrated the relevance of using CT images and deep learning models to aid in the diagnosis of COVID-19. More recent studies have sought better solutions for this scenario [16,17]. Despite the higher cost

of CT compared to radiography (CXR), it can demonstrate the characteristics for the screening of COVID-19 [17] more clearly. Works such as [18] have shown that ground-glass opacity and consolidation are usually not identified in computed radiography images, but can be more easily identified in CT.

Another technique that has been gaining importance in the scientific community is the variational autoencoders, a specific case of the unsupervised learning, in which several works have shown promising results for biomedical image processing [19, 20]. Thus, it is a consensus that the current scenario has marked the spread use of computational techniques for health, especially in the processing of medical images [13] related to COVID-19.

Likewise, the use of models based on *fuzzy* logic, a theory initially proposed in [21], which deals with fuzzy sets tomodel uncertainties, has shown important results in several applications, including the medical area [22]. Regardingthe use of CT images modeled by *Fuzzy* theory and *Deep Learning* algorithms, some studies have demonstrated its effectiveness when performed to classify images of COVID-19 [23].

As COVID-19 is relatively recent, the number of databases sufficient to train appropriate deep networks is limited. In this context, transfer learning [24] techniques have been attractive for problems with few data and limited hardware structure for training the algorithms [25].

In this work, a method for classifying CT images of COVID-19 using *Deep Learning* techniques, and unsupervised algorithms based on an ensemble structure is proposed. For feature extraction, we exploit the good capacity of Deep Learning by implementing variational autoencoder [19] and transfer learning. The feature extraction is performed in a specialist way, in which one data class is confronted with the others. With that, custom feature vectors for each classare extracted. Later, they are thus combined (concatenated) using an ensemble alike method, and finally presented to unsupervised classification methods, specifically, *k-means* and *Fuzzy C-Means* (FCM).

1.1 Main Contributions

This work presents the processing of CT images for the diagnosis of COVID-19 in unsupervised learning scenarios, which, in the current literature, are less investigated than the supervised learning methods. Two system architectures are implemented and compared to evaluate different feature extraction structures. In addition, ensemble structures are used to improve model generalization.

1.2 Organization

This research is organized as follows: Section 2 presents the main theoretical concepts that involve the proposed system. Section 3, presents the related works. Section 4 presents the proposed method, as well as the description of the adopted database. Section 5 presents the results and an in-depth discussion. Final considerations and future work are presented in Section 6.

2 Theoretical Background

2.1 Convolutional Neural Network (CNNs)

Deep Learning techniques, such as the Convolutional Neural Network, have been successfully applied to image processing, which makes their use promising for medical image analysis. The Convolutional Neural Network is a multi-layered network proposed by [26] that contain structures capable of extracting features for pattern recognition in image data analysis [27]. Since then, several CNNs have been proposed, each one with its own structure.

In CNNs, the states in each layer are organized according to the grid structure, so each layer of the convolutional network is a three-dimensional network structure, which has height, width, and depth [28].

The work reported in [29] proposed a Convolutional Neural Network based on ResNet [10], which was used in present work through the transfer of learning process for feature extraction in the first scenario. A brief description of this architecture is presented in the next section

2.1.1 ResNet (Residual Network)

The basic idea of ResNet is to exploit residual blocks. Residual blocks were proposed to solve the gradient explosion problem, which later converged to the development of ResNet [10]. The main functionality of residual blocks is in the perspective of learning through residual mapping. Basically, ResNet is characterized by the stacking of several residual blocks, which led to the creation of several networks of residual blocks, for example ResNet-50, which meansresidual of 50 layers with hop connection.

In addition to ResNet, the literature has several CNNs, such as: Visual Geometry Group (VGG) [30], Dense Convolutional Network (DenseNet) [31], GoogLeNet [32], Inception [33], Xception [34] among others. These architectures were trained on the *imagenet* [35] dataset and are available for the transfer learning process.

2.1.2 Transfer Learning

Transfer learning is a machine learning method where a model developed for a task is reused as the starting point or as preprocessing stage for a model on a second task [24].

The basic idea of CNNs is that through convolutional layers, general and hidden features can be extracted from images, such as edges, textures, shapes and composition of objects, while the last layers are able to identify specific image features such as eyes, wheels, lung, among others (depending on the problem in question). In this sense, with the use of transfer learning, the first layers of a given CNN are frozen (responsible for detecting edges, for example), and only the last layers are trained. These last are responsible for adapting to the desired situation.

Thus, the objective of transfer learning is to improve the performance of the model by transferring information from a related domain to be adapted to the desired task. Transfer learning has been used mainly when you have a limited dataset for training.

2.2 Variational Autoencoder

Considered in the literature as a feature extraction and data augmentation method, the Variational Autoencoder (VAE) is a generative model based on variational Bayesian learning, using a deep learning framework [19, 36]. In general, VAE extracts latent values from input variables to generate new information.

Considering a data set with N independent and identically distributed samples (i.i.d.) for a continuous variable x, the VAE is designed to estimate the probabilities $P(X)$, so that real samples with high probability and random noise with low probability are obtained [36]. According to [37], in the general case, to generate real data it is assumed that this is a random process consisting of two points: (i) the latent and continuous variable z is generated from *a priori* distributions $p(z; \theta)$; and (ii) the observed data x are results of the conditional distribution $p(x|z; \theta)$, as described in the Bayesian theory, where z is a latent variable, θ is the value of the parameters and $p(z|x)$ is an intractable posteriori in the general case.

Thus, the inference of the VAEs is performed by maximizing a variational lower limit $L(\theta, \varphi; xi)$, which can be derived by [37]:

$$L(\theta, \phi; xi) = -KL(q(z|x_i; \phi) \parallel p(z; \theta)) + E_q(z|x_i; \phi)[\log p(x_i|z; \theta)] \quad (1)$$

where the parameters ϕ and θ are the learned weights of the VAE.

Conventionally, the *a priori* distribution $p(x; \theta)$ is assumed to be multivariate Gaussian [38], hence the *a posteriori* $p(x|x_i; \theta)$ is an approximate Gaussian with approximately diagonal covariance [37]. Then, $L(\theta, \varphi; x_i)$ is expressed by:

$$L(\theta, \phi; x_i) \cong \frac{1}{2}\sum_{j=1}^{n}\left(1 + log\sigma^2{}_{i,j} - \mu^2{}_{i,j} - \sigma^2{}_{i,j}\right) + \frac{1}{L}\sum_{l=1}^{l} logp\,(x_i \vee z_i; \theta) \quad (2)$$

where μ and σ^2 are the mean and variance of the VAE encoder parameters, respectively. Furthermore, J refers to dimensionality and L to the sample size.

2.3 Fishers' Discriminant Ratio

The Fishers' Discriminat Ratio (FDR) [39] is a well known method for feature selection, which is very useful in pattern recognition systems for dimension reduction. The FDR cost vector function is expressed as:

$$\mathbf{F} = (\mu_1 - \mu_2)^2 \odot \frac{1}{\sigma_1^2 + \sigma_2^2} \quad (3)$$

where $F = [F_1, \ldots, F_L]^T$, is the "discriminant relevance" for each feature; L is the total number of features; μ_1 and μ_2, and σ_1 and σ_2 are the mean and variance of the feature vectors of classes 1 and 2, respectively; and refers to the *Hadamard* product [40]. The term in the numerator in (3) indicates how far the feature map distributions are from each other, while the denominator indicates how spread out these distributions are. Thus, the higher is the value of F, the greater the discriminating power of the feature.

2.4 *k-means*

The *k-means* algorithm described by [41, 42] aims to decisively partition a data set X into a certain number of c clusters. The algorithm basically works minimizing the within-cluster sum of squares given by equation (4), allocating each data sample $x_k \in \mathrm{R}$ $(k = 1, \ldots, N)$ to its nearest cluster:

$$J_{KM}(X; V) = \sum_{n=1}^{c} \sum_{k=A_i} \| x_k - v_i \|^2 \quad (4)$$

where $v_i \in R^n$, $(i = 1, \ldots, c)$ is the mean of the data vectors inside cluster *i*, given by equation (5), and A_i is the setof samples that are closer to the i_{th} cluster center than to the others.

$$v_i = \frac{1}{N_i} \sum_{k=1}^{N_i} x_j, x_i \in A_i, \quad (5)$$

where N_i is the number of samples in A_i. This method has no guarantee to converge to a global optimum, due toits initialization that uses random samples to measure the initial Means.

2.5 Fuzzy C-Means

Basically, the algorithm *k-means* works by assigning data to centroids, so [42] proposed an algorithm based on *k-means* where it is possible to handle uncertainties using the membership degree, the FCM algorithm, which is one of the widely used algorithms for *Fuzzy* classification [43].

In general, the FCM aims to partition the data in such a way that intra-group samples are more similar to each other, and inter-group samples are less similar, generating a degree of pertinence associated with a data set *X* in a certain number of *clusters*. This process occurs via an objective function, given by:

$$J_{FCM}(X; U, V) = \sum_{i=1}^{c} \sum_{k=1}^{N} \left(\xi_{k,i}\right)^m \| x_k - v_i \|^2 \quad (6)$$

where $x_k \in R^n$, $(i = 1, \ldots, N)$ represents the samples; $v_i \in R^n$, $(i = 1, \ldots, c)$ is the cluster center, which can be defined by:

$$v_i = \frac{\sum_{k=1}^{N} (\xi_{k,i})^m . x_k}{\sum_{k=1}^{N} (\xi_{k,i})^m} \quad (7)$$

where *n* is the number of variables; *c* is the number of clusters; *m* is the fuzziness constant; and ξ_{ki}, is the membership degree of the k_{th} sample in the i_{th} cluster:

$$v_i = \begin{bmatrix} \xi_{11} & \cdots & \xi_{1i} & \cdots & \xi_{1c} \\ \vdots & \ddots & & \vdots & \vdots \\ \xi_{k1} & \cdots & \xi_{ki} & \cdots & \xi_{kc} \\ \vdots & \cdots & \vdots & \ddots & \vdots \\ \xi_{N1} & & \xi_{Ni} & \cdots & \xi_{Nc} \end{bmatrix} \quad (8)$$

subject to the following restrictions: $\sum_{i=1}^{N} \xi_{nk} = 1 \ \forall n;$ and $0 < \sum_{i=1}^{K} \xi_{nk} < 1 \forall k$. The elements of the partition matrix are given by:

$$\xi_{ki} = \frac{1}{\sum_{j=1}^{c} \frac{D_{ki}}{D_{kj}}^{\frac{2}{m-1}}}, \quad (9)$$

where D_{ki} is the square distance between x_k and v_k, given by:

$$\| x_k - v_i \|^2 = D_{k,i}^2 = (x_k - v_i)^T (x_k - v_i). \quad (10)$$

The centers will converge to a position in the feature space where the partition matrix presents a minimal variation, i.e. when $||\Delta U|| \leq \epsilon$.

2.6 Self Organizing Maps

Self Organizing Maps (SOM) is an unsupervised machine learning method designed to map a high dimension dataset into a low dimension feature map [44]. The network is trained with a competitive algorithm, where the closest weights are updated towards the sample feature vectors. Given a set of samples like $x = [x_1, x_2, \ldots, x_M]$ (where M represents the total

number of features), the algorithm calculates the distance between every single sample vector to each neuron, aiming to find the best match. The learning rule of SOM comprises to update a set of neurons within a certain neighborhood ($N_\phi(d)$), which can be done by:

$$\begin{cases} w_{\phi|}^{(t)} = w_\phi^{(t-1)} + \lambda(x_M^{(t)} - w_\phi^{(t-1)}, if\ w_\phi \in N_\phi^t \\ w_\phi^{(t)} = w_\phi^{(t-1)}, otherwise \end{cases} \quad (11)$$

where λ is the learning rate, and t represents the iteration.

3 Related Work

Much of the research done in the area of machine learning applied to COVID-19 image classification can be summarized as a feature extractor followed by a nonlinear classifier. The state-of-the-art literature review includes transfer learning research and expert models. This review section is selective and not exhaustive; therefore, it basically aims to highlight representative approaches in this context.

Recently, several works were developed in which promising results were found. These algorithms usually employ a classifier based on convolutional neural networks. The work reported in [45] used the Resnet-50 model through transfer learning to classify 5941 images from 2839 patients into four classes: normal, bacterial pneumonia, viral pneumonia and COVID-19, resizing was also adopted (pre-processing) of the images. This approach reached an average accuracyof 96.23% with only 41 epochs.

Some works have compared classification performances with and without the use of transfer learning. In [46], the authors used a CNN model and achieved an accuracy of 91%, without the use of data transfer learning, to differentiate between COVID-19 and non-COVID-19. This same study used transfer learning and the accuracy increased to 94% in differentiating between COVID-19 and non-COVID-19. Among the contributions of this work, the good performance of the model with transfer learning technique stands out.

In addition to transfer learning techniques, the preprocessing stage has also gained relevance in the analysis of COVID-19 images [47]. The work reported in [48] used transfer learning through the COVIDNet-CT model, which isbased on ResNet, and obtained a validation accuracy of 94.9% and a test accuracy of 88.89%, for the classes COVID-19, Pneumonia and Healthy. The model employed important preprocessing stages comprising to region of interest (RoI) extraction, normalization and image resizing. This literature review shows the relevance of extracting features via deep learning models. This work contributes by combining different feature extraction techniques with expert models to classify CT images of COVID-19.

4 Proposed Approach

The proposed approach consists of two ensemble structures based on unsupervised algorithms, as shown in Figure(1). Basically, the structures consist of three steps: feature extraction, feature selection and classification.

The first approach (upper left in Figure (1)) uses three pretrained models, developed specifically for COVID-19 image classification (COVIDNet-CT [29, 49]). These models were used to extract the feature vectors from the images, using a transfer learning approach, in which the outputs of the last convolutional layer of the models (flattened in one dimensional layer) are used. Two models provided 176 features and one model 412. The outputs are then concatenated, totaling 764 features. Thus, each processed image is represented by a vector of 764 features.

The second approach (upper right in Figure (1)) used Variational Autoencoder models to map the data into a latent space, which remains at the model bottleneck. After training the Variational Autoencoder, it is able to extract a reduced feature vector from each image. In this case, a Variational Autoencoder model was trained for each of the classes consisting of the following scenarios (COVID-18 vs (Other diseases and Healthy), Other diseases vs (COVID-19 and Healthy) and (Healthy vs (COVID-19 and Other diseases)). Note that each scenario is proposed to identify a class, through binary classification, hence the name expert class. With this strategy, the model is trained to identify patterns of a certain class. The three models were trained with a space 256 latent features[1] From there, VAE modelswere used to map all the images of the three classes to a single latent vector, obtained by concatenation of the outputsinto a vector with a total of 768 of features.[1]Following an intermediate latent space to map the data [50].

The final common step (at the center bottom in Figure (1)) uses FDR criterion for dimension reduction, decreasing the number of features to five for the k-means algorithm, which was the number of features such that the algorithm performed better. For the FCM and SOM algorithms, the number of features was not reduced with FDR, since it did not lead to better results. Thereby, this resulting feature vector is presented to the unsupervised classifiers FCM, k-means and SOM. Finally, in the operational stage, the distances from the test samples to the cluster centers are used as metric for final classification.

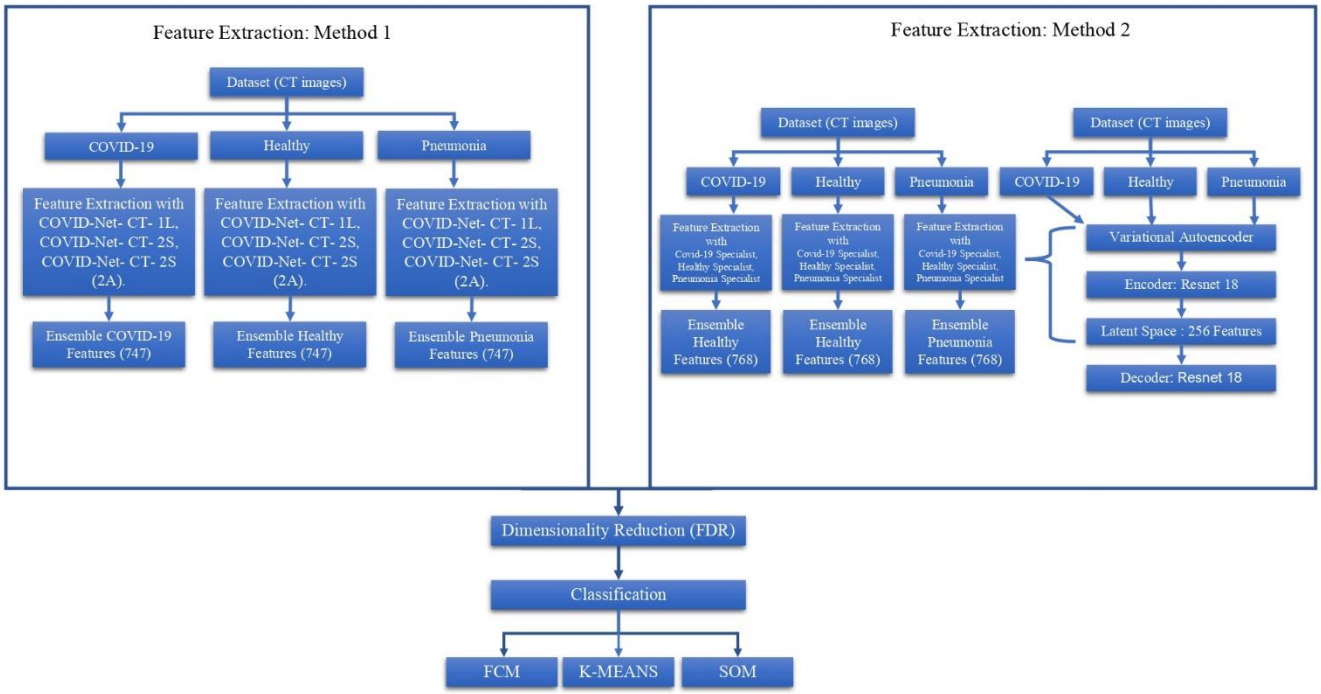

Figure 1: General model proposed, with feature extraction via modified ResNet convolutional neural network and variational autoencoder.

4.1 Database

As it is a respiratory disease, acute SARS-COV-2 infection is highly cytopathic, that is, it can cause damage to the alveolar structures of the lung, which can lead to extensive lung damage [51]. Thus, the lung is the most affected organ, featuring respiratory symptoms and changes that can be identified by computerized medical images.

For lesions caused by SARS-COV-2 to the lung, it is possible through computed tomography (CT) to identify abnormalities that may raise suspicion of probable infection by COVID-19. The main findings on chest CT include ground-glass opacity, vascular enlargement, and bilateral abnormalities.

Thus, a data set with CT scans in PNG format was used, which are divided into: 758 CT scans for healthy patients(15 CT scans on average per patient). 2.168 CT scans for patients infected with SASR-CoV-2 (on average 27 CT scans per patient) and 1.247 CT scans for patients with other pulmonary directions (on average 16 CT scans per patient) [52].

Figure (2) shows chest CT sample examples of each of the classes, in Figure (2.a), COVID-19 exam is shown, where it can be observed the whitish regions, in contrast to what is shown in Figure (2.b) for a healthy patient. Besides, as shown in (Figure (2.c) other diseases can also be confused with COVID-19, as CT images also exhibit whitish regions.

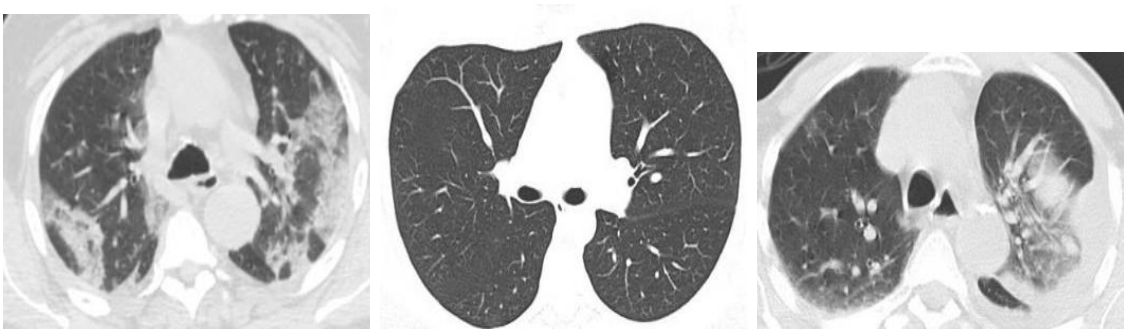

(a) Patient with COVID-19 (b) Healthy patient (c) Patient with other lung diseases

Figure 2: CT scan of database samples.

With the objective of feasibility and generalization of the proposed approach, the system will be trained and tested through *K-fold* cross-validation procedure [53, 54].

5 Results and Discussions

5.1 Data Cleanup

For scenario 1, the extraction of image attributes was performed based on the layer before the dense layer of the network, totaling a set of 764 attributes, being 176 of two models with a lower number of parameters and 412 ofanother model with a higher number of parameters. A small part of these attributes was null and, when applying the *Fisher* ratio, the results were interpreted as non-numerical, as it is a mathematical indeterminacy. To resolve this issue, the attributes were removed, leaving 747 attributes per sample.

5.2 Numerical Results

Seeking to analyze this divergence between the model and the classification in the databases, three different scenarioswere created for a more detailed analysis. Confronting the COVID-19 and Healthy, COVID-19 and Other Diseases,and finally COVID-19, Other Diseases and Healthy.

5.2.1 FCM, k-means and SOM via transfer learning

The analysis of the scenarios was initially divided into two sections, the Tables 1, 2 and 6 summarize the information on the binary classification COVID-19 vs Healthy and COVID-19 vs Other Diseases for FCM, k-means and SOM, respectively, in terms of accuracies for both train and testing data sets. Similarly, Tables 4, 5 and 6 present the results of the multiclass classification COVID vs Healthy vs Others. With the objective of verifying the best scenario, several configurations were analyzed, thus the number of clusters was varied from 2 to 12 and the total amount of attributesper sample was maintained.

To measure the accuracy of the FCM algorithm, it was used the Mahalanobis distance from every sample to the center, and for k-means and SOM, it was used the Euclidean distance to the cluster centers/neurons.

Table 1: Classifier *Fuzzy C-Means* for binary scenario.

Clusters	**COVID-19 × Healthy**		**COVID-19 × Others**	
	train accuracy	*test accuracy*	*train accuracy*	*test accuracy*
2	84.3 ± 6.9	85.6 ± 12.9	68.9 ± 2.2	63.8 ± 5.2
4	42.7 ± 17.6	52.1 ± 20.9	33.3 ± 9.5	33.9 ± 9.3
6	27.8 ± 18.4	39.1 ± 31.3	8.9 ± 13.4	10.6 ± 11.7
8	10.9 ± 13.3	9.4 ± 12.9	22.9 ± 21.1	22.4 ± 20.4
12	8.8 ± 15.2	13.0± 23.1	12.4 ± 3.3	13.6 ± 4.9

Table 2: Classifier *k-means* for binary scenario.

Clusters	**COVID-19 × Healthy**		**COVID-19 × Others**	
	train accuracy	*test accuracy*	*train accuracy*	*test accuracy*
2	88.2 ± 0.8	90.2± 7.7	70.6 ± 0.7	66.4 ± 7.0
4	43.4 ± 16.4	44.0 ± 23.3	36.4 ± 3.8	35.3 ± 7.9
6	25.6± 12.9	26.4 ± 18.6	22.9 ± 6.6	21.7 ± 7.6
8	20.1 ± 12.3	23.5 ± 15.0	19.5 ± 3.1	18.8 ± 8.0
12	15.8 ± 6.8	19.8± 11.1	12.4 ± 3.3	13.6 ± 4.9

Table 3: Classifier *Self-Organizing Maps* for binary scenario.

Clusters	**COVID-19 × Healthy**		**COVID-19 × Others**	
	train accuracy	*test accuracy*	*train accuracy*	*test accuracy*
2	87.3 ± 0.8	89.3 ± 7.3	69.5 ± 0.6	65.0 ± 5.5
4	60.2 ± 4.1	57.0 ± 15.5	45.1 ± 2.2	44.1 ± 8.2
6	20.8 ± 5.0	16.4 ± 6.4	26.9 ± 0.4	27.9 ± 6.3
8	18.8 ± 3.8	10.3 ± 4.1	19.6 ± 0.9	19.9 ± 4.7
12	11.3 ± 2.1	9.8± 4.3	11.6 ± 0.6	12.1 ± 2.9

Table 4: Classifier *Fuzzy C-Means* for multiclass scenario.		
Clusters	**COVID-19 × Others × Healthy**	
	train accuracy	*test accuracy*
3	55.9 ± 4.8	56.4 ± 8.8
6	29.6 ± 17.1	32,2 ± 16.4
9	28.4 ± 19.7	28.5 ± 19.3
12	13.7 ± 15.3	14.2 ± 15.6

Table 5: Classifier *k-means* for multiclass scenario.		
Clusters	**COVID-19 × Others × Healthy**	
	train accuracy	*test accuracy*
3	50.8 ± 5.3	55.1 ± 8.1
6	28.1 ± 2.8	27.3 ± 5.4
9	18.4 ± 4.8	18.5 ± 6.2
12	14.2 ± 4.5	14.3 ± 4.3

Table 6: Classifier Self-Organizing Maps for multiclass scenario.		
Clusters	**COVID-19 × Others × Healthy**	
	train accuracy	*test accuracy*
3	60.2 ± 0.7	61.4 ± 6.0
6	28.6 ± 0.4	29.7 ± 3.3
9	15.3 ± 0.4	16.6 ± 3.2
12	10.6 ± 0.2	13.4 ± 3.3

For the binary classification (Tables 1, 2 and 3), the increase of the number of cluster led to the decreasing of the accuracy, in which two clusters was the best configuration for all clustering algorithms. This behaviour is also verifiedin the multiclass classifier, according to Tables 4, 5 and 6. In these last cases, three clusters scenario was the best value, since three classes (COVID-19, Other diseases and Healthy) were considered.

In general, the result obtained by the clustering algorithms was similar. By varying the set of attributes selectedby the criterion of Fisher's discriminant ratio for the algorithms C-Means and SOM, the performances were better when all the attributes extracted by the convolutional models were used (except for null values). In the algorithm *k-means* there was a need to use a smaller number of attributes, since the result for the total set of attributes presented a lower performance in relation to the scenario in which a greater number of attributes was used.

Other works in the literature also make use of the techniques studied here, such as transfer learning for feature extraction. The work reported in [55] used CT images for classification between COVID-19 and non-COVID, themodel performance for the COVID-19 class was 98.68% accuracy and 99.20% sensitivity. These results are superior to those achieved by the proposed models, however, this method was developed to identify COVID-19, while the proposed method classifies three classes: COVID-19, Healthy and Other diseases.

The work reported in [56] used transfer learning from DenseNet201, ResNet50, VGG16 and Xception convolutional networks, and the classifiers support vector machine, random forest, decision tree and k-nearest neighbors (KNN). A performance of 100% was found using features taken from DenseNet201 and the KNN classifier. This result suggests that other classifiers combined with different CNN must be considered to improve the performance of the proposed system.

5.2.2 FCM, k-means and SOM with Variational Autoencoder

The second scenario analyzed deals with the extraction of features via Variational Autoencoder, using the training configuration described in the proposed methods section. The results are summarized in Tables 7, 8 and 9 for the binary classification, and Tables 10, 11 and 12 for the multiclass classification. An interesting aspect of this scenario is the importance of specialist classes.

In general, both for the binary classification and for the multiclass classification, the results have a behavior like that presented in the first scenario.

Table 7: Classifier *FCM* for binary scenario.				
Clusters	**COVID-19 × Healthy**		**COVID-19 × Others**	
	train accuracy	*test accuracy*	*train accuracy*	*test accuracy*
2	96.3 ± 3.4	92.1 ± 5.4	63.6 ± 3.5	58.2 ± 6.6
4	42.1 ± 13.3	41.3 ± 14.7	29.6 ± 4.3	34.1 ± 8.4
6	22.2 ± 11.8	21.8 ± 11.5	21.1 ± 4.3	20.9 ± 5.2
8	15.8 ± 7.4	20.1 ± 11.7	15.7 ± 7.1	16.7 ± 12.5
12	16.1 ± 7.2	16.7 ± 7.4	7.1 ± 4.1	5.6 ± 3.2

Table 8: Classifier *k-means* for binary scenario.				
Clusters	**COVID-19 × Healthy**		**COVID-19 × Others**	
	train accuracy	*test accuracy*	*train accuracy*	*test accuracy*
2	95.1 ± 4.1	95.9 ± 3.9	64.1 ± 4.3	58.6 ± 6.5
4	55.4 ± 20.1	52.9 ± 21.6	30.6 ± 2.6	30.6 ± 7.7
6	35. 3 ± 9. 7	36.3 ± 13.7	23.8 ± 3.3	27.4 ± 11.7
8	24.6 ± 10.3	25.9 ± 12.5	16.8 ± 3.2	15.9 ± 6.2
12	14.7 ± 5.3	16.6 ± 7.1	10.2 ± 2.3	10.2 ± 2.9

Table 9: Classifier *Self-Organizing Maps* for binary scenario.				
Clusters	**COVID-19 × Healthy**		**COVID-19 × Others**	
	train accuracy	*test accuracy*	*train accuracy*	*test accuracy*
2	95.3 ± 5.5	95.9 ± 5.2	63.9 ± 3.4	58.2 ± 6.0
4	38.9 ± 6.4	40.1 ± 9.5	27.4 ± 1.6	28.0 ± 7.9
6	25.2 ± 7.5	28.0 ± 11.3	17.6 ± 1.9	18.0 ± 12.1
8	18.4 ± 4.9	19.5 ± 10.2	13.8 ± 1.7	15.3 ± 12.3
12	11.3 ± 2.9	10.8± 4.8	8.6 ± 0.9	9.4 ± 11.1

Table 10: Classifier *FCM* for multiclass scenario.		
Clusters	**COVID-19 × Others × Healthy**	
	train accuracy	*test accuracy*
3	53.1 ± 7.9	55.9 ± 9.0
6	26.9 ± 8.7	30.1 ± 6.5
9	17.8 ± 5.4	19.4 ± 6.1
12	14.5 ± 4.7	13.9 ± 5.2

Table 11: Classifier *k-means* for multiclass scenario.		
Clusters	**COVID-19 × Others × Healthy**	
	train accuracy	*test accuracy*
3	52.9 ± 8.5	54.8 ± 9.6
6	27.0 ± 6.2	30.6 ± 7.1
9	16.8 ± 5.3	16.4 ± 7.2
12	14.6 ± 4.7	14.6 ± 7.4

Table 12: Classifier Self-Organizing Maps for multiclass scenario.		
Clusters	**COVID-19 × Others × Healthy**	
	train accuracy	*test accuracy*
3	55.3 ± 6.8	57.9 ± 7.3
6	21.6 ± 4.8	20,6 ± 5.1
9	13.6 ± 2.7	16.4 ± 4.8
12	10.2 ± 2.6	11.8 ± 6.2

An interesting result is the training and testing accuracy for the binary classification considering two clusters, it is observed that the results were above 90% for both classifiers. Thus, it is observed that these results can be compared to those obtained by [19] that also used unsupervised learning to classify COVID-19 images.

Analyzing the two considered scenarios (both for binary classification and for multiclass) the combination of characteristics via variational autoencoders presented the best accuracy result for the "ideal" number of clusters.

As discussed, [57] from a clinical point of view, other performance measures, such as sensitivity and specificity, ensuremore reliable analyses, especially regarding the rate of false negatives and false positives. As we cannot diagnose a COVID-19 positive patient as negative, the patient may return to the community, believing they are COVID-19 free,which leads to community transmission of the disease. When we diagnose too many COVID-19 negatives as positives, it increases the burden on the healthcare system and causes public panic.

5.3 Graphical results

5.3.1 FCM, k-means and SOM via transfer learning

For the first proposed method, using the transfer learning technique with the COVID-Net models [29], was used the Fisher Discriminant Ratio to perform the dimensionality reduction, that allowed a optimization regarding the model complexity. The first analysis was meant to cluster COVID-19 patient samples from Healthy patient samples. Forthe testing set, the clusters centers, neurons and the samples in a 3D feature space, built considering the three most relevant features, according to the FDR criterion, are shown in Figures 3, 4 and 5.

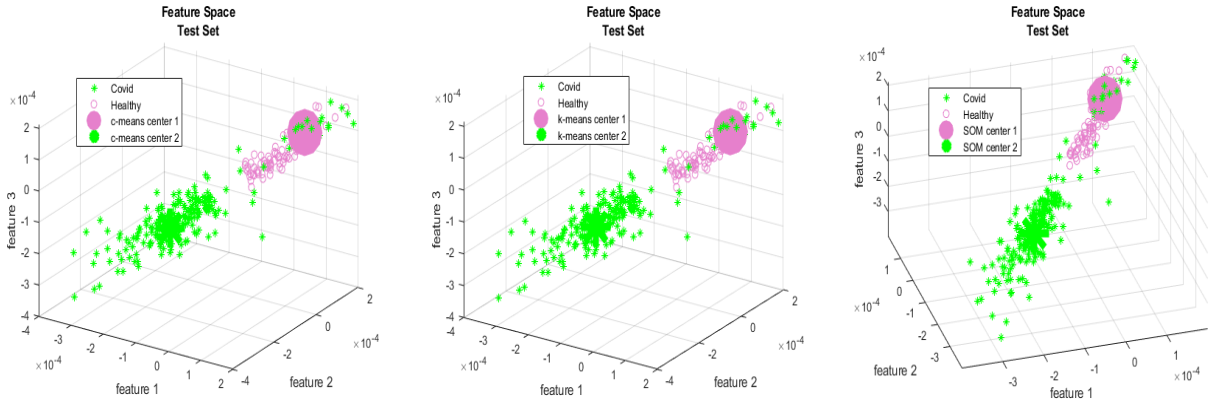

(a)FCM (b) *k-means* (c) *SOM*

Figure 3: COVID-19 vs. Healthy using: (a) FCM; (b) *k-means*; and (c) SOM classification models

.

As it can be observed in Figures 3(a), 3(b) and 3(c), the algorithms found clusters centers/neurons closer to each other, showing a slight difference between them, only observed when the image is zoomed in. The second analysis proposed (COVID-19 vs Others) does not perform as good as the first one, both methods showed a poor performancecompared with the first one. A possible reason for the lower performance would be due to the similarity between covid samples and other diseases samples. The feature space for FCM, k-means and SOM algorithms became as shown inFigure 4.

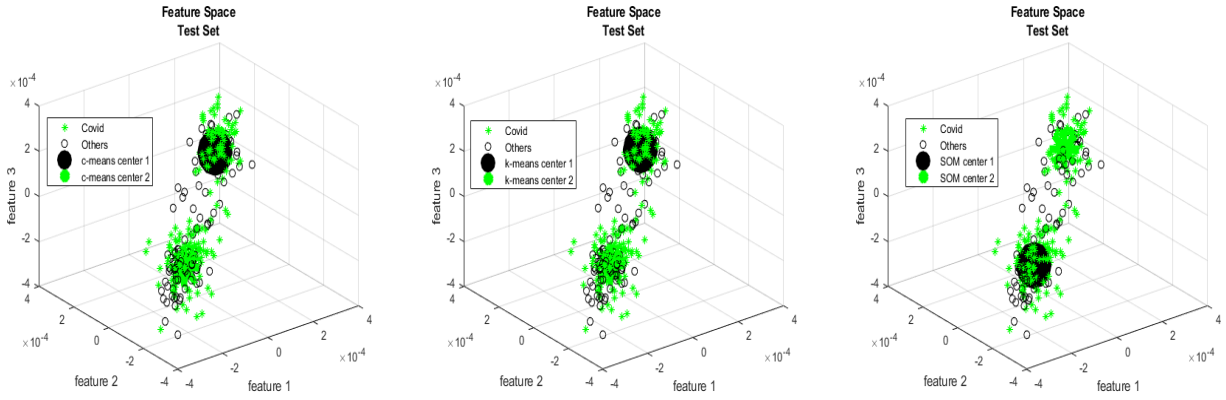

(a) *FCM* (b) *k-means* (c) *SOM*

Figure 4: COVID-19 vs. Others using: (a) FCM and (b) *k-means* and (c) SOM classification models.

The last analysis aimed to cluster all three classes, and as expected the clusters centers does not fit exactly whereit should be, mainly COVID-19 and others diseases samples, that shows more closer relation than COVID-19 and Healthy samples. The healthy cluster center appears to be the most separable one, as shown in Figure 5.

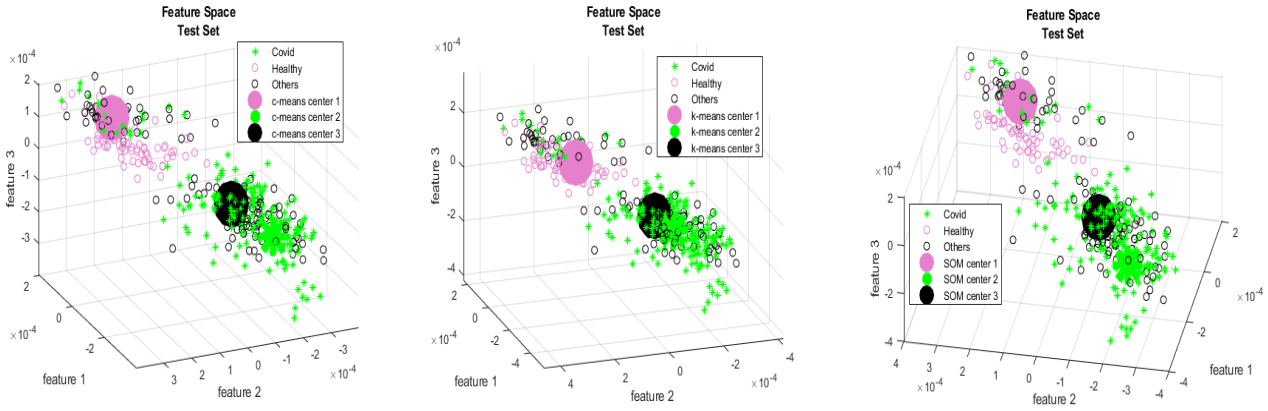

(a) *FCM* (b) *k-means* (c) *SOM*

Figure 5: COVID-19 vs. Healthy vs. Others using: (a) FCM and (b) *k-means* and (c) SOM classification models.

Considering that a Transfer Learning was performed in this first analysis, the feature extraction builds a goodfeature space for the first scenario (COVID-19 versus Healthy), a reasonable feature space for the second scenario (COVID-19 versus Others), and a poor quality feature space for the third scenario (COVID-19 versus Healthy versus Others). Also, considering an analysis from a model trained in another database, these models managed to extract the features from the images, in general.

5.3.2 FCM, k-means and SOM with Variational Autoencoder

For the second method we had three fully trained models, each one trained to recognize its own class, the so called specialists models. Variational Autoencoders are trained for each of the classes, with the trained models in hand, the entire data set is "passed" in each of the expert models, generating the final set of features.

After training the models to generate new samples, it becomes able to extract the samples features and compress itto a latent space usually called z space. To achieve this results the *Fisher* 's discriminant ratio was also used as in the first method. The first three features with the highest ratio were chosen to plot the latent space in three dimensions. First the analysis of COVID-19 against healthy samples was captured, and the output can be seen in Figure 6.

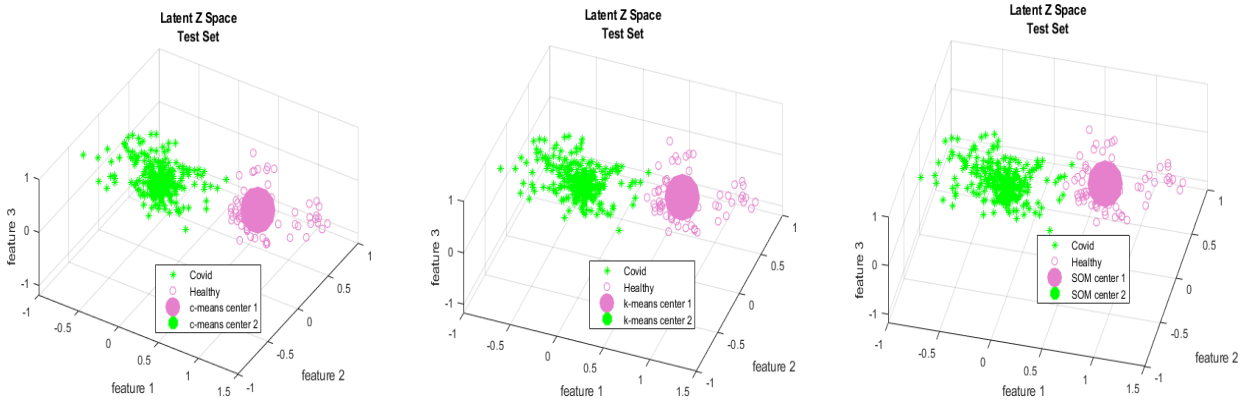

(a)FCM (b) *k-means* (c) *SOM*

Figure 6: COVID-19 vs. Healthy using: (a) FCM and (b) k-means and (c) SOM classification models.

The latent space or hidden space created by Variational Autoencoder models, shows a higher clustering level when compared with transfer learning method, as it was fitted in the data to acquire hidden features from the images. The clustering algorithms obtained high performance results in terms of classification. For the COVID-19 versus others diseases scenario, the graphical result wasn't good as the previous one, as it can be seen in the Figure 7.

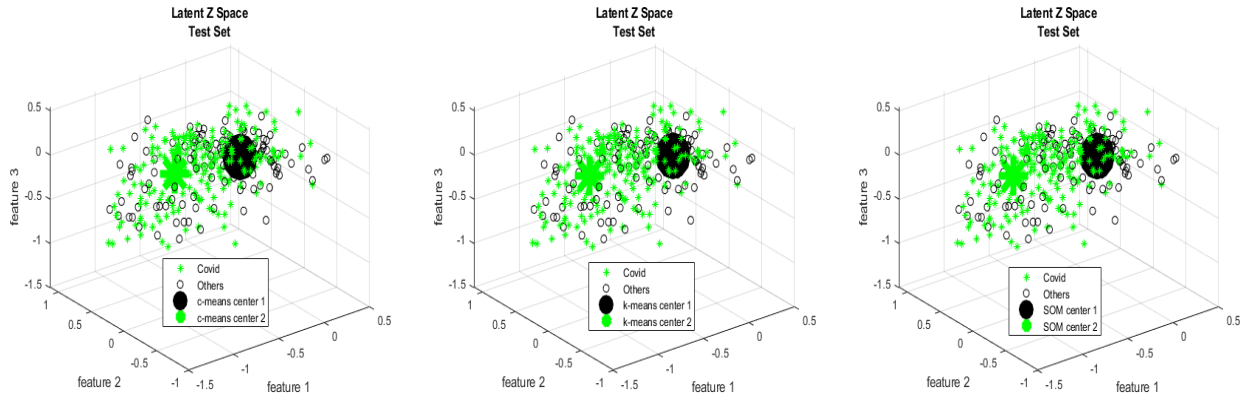

(a) *FCM* (b) *k-means* (c) *SOM*

Figure 7: COVID-19 vs. Others using: (a) FCM and (b) *k-means* and (c) SOM classification models.

As it was observed at the first method, the COVID-19 versus other diseases has a lower clustering level, when dealing with the latent feature space, possible due to its similarity on the lesions patterns in the images, giving a more similar latent space. For the last analysis, considering all the three classes, the healthy class seems to be the most separable again, considering the feature space.

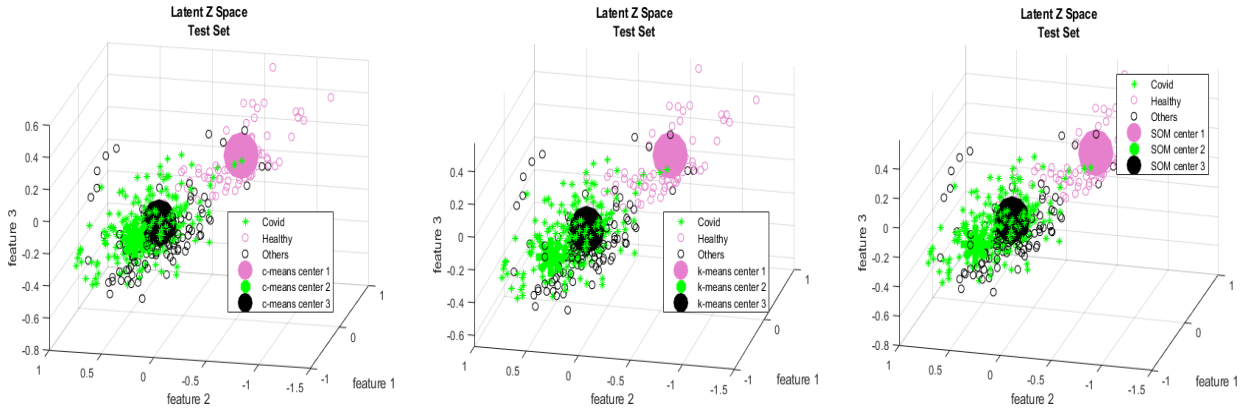

(a) *FCM* (b) *k-means* (c) *SOM*

Figure 8: COVID-19 vs Healthy vs Others using: (a) FCM and (b) *k-means* and (c) SOM classification models.

The latent feature space created by the VAE, showed a better clustering level when dealing with the first analysis, COVID-19 against healthy samples, but an equivalent performance in the other comparisons.

6 Conclusion and Future Works

The COVID-19 screening through computational techniques has become an important tool to help health professionals. Unlike most works in the literature, this work proposes unsupervised learning since unlabeled data can be used. The proposed system also relies on the use of ensemble techniques, which can contribute to a better generalization of the model. The proposal was used to evaluate two methodological scenarios and the results were competitivewith works in the literature, with accuracies varying from around 52% to 95% in testing data. The best results were achieved with the extraction of features via variational autoencoder, a reason for that would be because the extractormodel was designed by considering the used data set, instead of using a transfer leaning approach.

In addition, in future work, it is expected to include other databases, comparing with other supervised learning classifiers. Another contribution is working in the area of unsupervised online learning.

7 Acknowledgment

The present authors would like to thank the Coordination for the Improvement of Higher Education Personnel-Brazil (CAPES)- Financing Code 001, National Council for Scientific and Technological Development (CNPq), Foun- dation for Research Support of the State of Minas Gerais (FAPEMIG) and Foundation for Research Support of the State of Rio de Janeiro (FAPERJ) for financial support. As well as a thank you to the team that develops the project of the Telemedicine public notice (Emergency Selection Notice III CAPES - Telemedicine and Medical Data Analysis), for the fruitful discussions regarding this work.

8 References

[1] F. Zheng, C. Liao, Q.-h. Fan, H.-b. Chen, X.-g. Zhao, Z.-g. Xie, X.-l. Li, C.-x. Chen, X.-x. Lu, Z.-s. Liu et al. "Clinical characteristics of children with coronavirus disease 2019 in Hubei, China". Current medical science, vol. 40, no. 2, pp. 275–280, 2020.

[2] T. Kobayashi, S.-m. Jung, N. M. Linton, R. Kinoshita, K. Hayashi, T. Miyama, A. Anzai, Y. Yang, B. Yuan, A. R. Akhmetzhanov et al. "Communicating the risk of death from novel coronavirus disease (COVID-19)". Journal of clinical medicine, vol. 9, no. 2, pp. 580, 2020.

[3] M. Park, R. S. Thwaites and P. J. Openshaw. "COVID-19: Lessons from SARS and MERS". European journalof immunology, vol. 50, no. 3, pp. 308–311, 2020.

[4] Y. Pan, H. Guan, S. Zhou, Y. Wang, Q. Li, T. Zhu, Q. Hu and L. Xia. "Initial CT findings and temporal changes in patients with the novel coronavirus pneumonia (2019-nCoV): a study of 63 patients in Wuhan, China". European Radiology, vol. 30, no. 6, pp. 3306–3309, Jun 2020.

[5] B. Visser and R. Van Brakel. Tracing The Tracers 2021 report: Automating COVID responses: The impact of automated decision-making on the COVID-19 pandemic. Algorithm Watch, 12 2021.

[6] H. Bastani, K. Drakopoulos, V. Gupta, J. Vlachogiannis, C. Hadjicristodoulou, P. Lagiou, G. Magiorkinis, D. Paraskevis and S. Tsiodras. "Efficient and Targeted COVID-19 Border Testing via Reinforcement Learn-ing". Nature, 2021.

[7] L. Li, L. Qin, Z. Xu, Y. Yin, X. Wang, B. Kong, J. Bai, Y. Lu, Z. Fang, Q. Song, K. Cao, D. Liu, G. Wang, Q. Xu, X. Fang, S. Zhang, J. Xia and J. Xia. "Using Artificial Intelligence to Detect COVID-19 and Community-acquired Pneumonia Based on Pulmonary CT: Evaluation of the Diagnostic Accuracy". Radiology, vol. 296, no. 2, pp. E65–E71, 2020.

[8] I. H. Sarker. "Deep learning: a comprehensive overview on techniques, taxonomy, applications and research directions". SN Computer Science, vol. 2, no. 6, pp. 1–20, 2021.

[9] R. Yamashita, M. Nishio, R. K. G. Do and K. Togashi. "Convolutional neural networks: an overview and application in radiology". Insights into imaging, vol. 9, no. 4, pp. 611–629, 2018.

[10] K. He, X. Zhang, S. Ren and J. Sun. "Deep residual learning for image recognition". In Proceedings of the IEEE conference on computer vision and pattern recognition, pp. 770–778, 2016.

[11] M. Tan and Q. Le. "Efficientnet: Rethinking model scaling for convolutional neural networks". In International conference on machine learning, pp. 6105–6114. PMLR, 2019.

[12] C. Pinto, J. Furukawa, H. Fukai and S. Tamura. "Classification of Green coffee bean images basec on defect types using convolutional neural network (CNN)". In 2017 International Conference on Advanced Informatics, Concepts, Theory, and Applications (ICAICTA), pp. 1–5, 2017.

[13] F. Shi, J. Wang, J. Shi, Z. Wu, Q. Wang, Z. Tang, K. He, Y. Shi and D. Shen. "Review of artificial intelligence techniques in imaging data acquisition, segmentation, and diagnosis for COVID-19". IEEE reviews in biomedical engineering, vol. 14, pp. 4–15, 2020.

[14] S. Jin, B. Wang, H. Xu, C. Luo, L. Wei, W. Zhao, X. Hou, W. Ma, Z. Xu, Z. Zheng et al. "AI-assisted CT imaging analysis for COVID-19 screening: Building and deploying a medical AI system in four weeks". MedRxiv, 2020.

[15] K. Zhang, X. Liu, J. Shen, Z. Li, Y. Sang, X. Wu, Y. Zha, W. Liang, C. Wang, K. Wang et al. "Clinically applicable AI system for accurate diagnosis, quantitative measurements, and prognosis of COVID-19 pneumoniausing computed tomography". Cell, vol. 181, no. 6, pp. 1423–1433, 2020.

[16] I. Shiri, H. Arabi, Y. Salimi, A. Sanaat, A. Akhavanallaf, G. Hajianfar, D. Askari, S. Moradi, Z. Mansouri, M. Pakbin et al. "COLI-Net: Deep learning-assisted fully automated COVID-19 lung and infection pneumonia lesion detection and segmentation from chest computed tomography images". International journal of imaging systems and technology, vol. 32, no. 1, pp. 12–25, 2022.

[17] P. Chikontwe, M. Luna, M. Kang, K. S. Hong, J. H. Ahn and S. H. Park. "Dual attention multiple instance learning with unsupervised complementary loss for COVID-19 screening". Medical Image Analysis, vol. 72, pp.102105, 2021.

[18] M.Y. Ng, E. Y. Lee, J. Yang, F. Yang, X. Li, H. Wang, M. M.-s. Lui, C. S.-Y. Lo, B. Leung, P.L. Khong et al. "Imaging profile of the COVID-19 infection: radiologic findings and literature review". Radiology: Cardiothoracic Imaging, vol. 2, no. 1, 2020.

[19] R. F. Mansour, J. Escorcia-gutierrez, M. Gamarra, D. Gupta, O. Castillo and S. Kumar. "Unsupervised Deep Learning based Variational Autoencoder Model for COVID-19 Diagnosis and Classification". Pattern Recognition Letters, vol. 151, no. January, pp. 267–274 Contents, 2021.

[20] W. Zheng, L. Yan, C. Gou, Z.-C. Zhang, J. J. Zhang, M. Hu and F.-Y. Wang. "Learning to learn by yourself: Unsupervised meta-learning with self-knowledge distillation for COVID-19 diagnosis from pneumonia cases". International Journal of Intelligent Systems, vol. 36, no. 8, pp. 4033–4064, 2021.

[21] L. Zadeh. "Fuzzy sets". Information and Control, vol. 8, no. 3, pp. 338 – 353, 1965.

[22] A. Alzahrani, M. Bhuiyan, F. Akhter et al. "Detecting COVID-19 Pneumonia over Fuzzy Image Enhancementon Computed Tomography Images". Computational and Mathematical Methods in Medicine, vol. 2022, 2022.

[23] A. M. Tripathi and A. Mishra. "Fuzzy unique image transformation: Defense against adversarial attacks on deep COVID-19 models". arXiv, vol. 14, no. 8, pp. 1–11, 2020.

[24] R. Kundu, P. K. Singh, M. Ferrara, A. Ahmadian and R. Sarkar. "ET-NET: an ensemble of transfer learning models for prediction of COVID-19 infection through chest CT-scan images". Multimedia Tools and Applications, vol. 81, no. 1, pp. 31–50, 2022.

[25] A. Abbas, M. M. Abdelsamea and M. M. Gaber. "4S-DT: Self-Supervised Super Sample Decomposition for Transfer Learning with Application to COVID-19 Detection". IEEE Transactions on Neural Networks and Learning Systems, vol. 32, no. 7, pp. 2798–2808, 2021.

[26] Y. Lecun and Y. Bengio. "Convolutional Networks for Images, Speech, and Time-Series". The handbook of brain theory and neural networks, vol. 3361, no. November, pp. 1–14, 1998.

[27] M. Lin, Q. Chen and S. Yan. "Network in network". 2nd International Conference on Learning Representations, ICLR 2014 - Conference Track Proceedings, pp. 1–10, 2014.

[28] C. C. Aggarwal et al. "Neural networks and deep learning". Springer, vol. 10, pp. 978–3, 2018.

[29] H. Gunraj, A. Sabri, D. Koff and A. Wong. "COVID-Net CT-2: Enhanced deep neural networks for detection of COVID-19 from Chest CT images through bigger, more diverse learning". arXiv preprint arXiv:2101.07433, 2021.

[30] K. Simonyan and A. Zisserman. "Very deep convolutional networks for large-scale image recognition". arXiv preprint arXiv:1409.1556, 2014.

[31] G. Huang, Z. Liu, L. Van Der Maaten and K. Q. Weinberger. "Densely connected convolutional networks". In Proceedings of the IEEE conference on computer vision and pattern recognition, pp. 4700–4708, 2017.

[32] C. Szegedy, W. Liu, Y. Jia, P. Sermanet, S. Reed, D. Anguelov, D. Erhan, V. Vanhoucke and A. Rabinovich. "Going deeper with convolutions". In Proceedings of the IEEE conference on computer vision and pattern recognition, pp. 1–9, 2015.

[33] C. Szegedy, S. Ioffe, V. Vanhoucke and A. A. Alemi. "Inception-v4, inception-resnet and the impact of residual connections on learning". In Thirty-first AAAI conference on artificial intelligence, 2017.

[34] F. Chollet. "Deep learning with depthwise separable convolutions". In Proceedings of the IEEE Conference on Computer Vision and Pattern Recognition, pp. 1251–1258, 2017.

[35] J. Deng, W. Dong, R. Socher, L.-J. Li, K. Li and L. Fei-Fei. "Imagenet: A large-scale hierarchical image database". In 2009 IEEE conference on computer vision and pattern recognition, pp. 248–255. Ieee, 2009.

[36] H. Nishizaki. "Data augmentation and feature extraction using variational autoencoder for acoustic modeling".In 2017 Asia-Pacific Signal and Information Processing Association Annual Summit and Conference (APSIPA ASC), pp. 1222–1227, 2017.

[37] X. Chen, Y. Sun, M. Zhang and D. Peng. "Evolving Deep Convolutional Variational Autoencoders for Image Classification". IEEE Transactions on Evolutionary Computation, vol. 25, no. 5, pp. 815–829, 2021.

[38] S. Mandal, A. A. Jammal and F. A. Medeiros. "Assessing glaucoma in retinal fundus photographs using Deep Feature Consistent Variational Autoencoders". Preprints 2021, vol. 1, pp. 1–11, 2021.

[39] S. Theodoridis and K. Koutroumbas. Pattern recognition. Elsevier, 2006.

[40] D. D. Ferreira, A. S. Cerqueira, C. A. Duque and M. V. Ribeiro. "HOS-based method for classification of power quality disturbances". Electronics Letters, vol. 45, no. 3, pp. 183–185, 2009.

[41] V. C. Mota, F. A. Damasceno, E. A. Soares and D. F. Leite. "Fuzzy clustering methods applied to the evaluationof compost bedded pack barns". IEEE International Conference on Fuzzy Systems, pp. 1–6, 2017.

[42] J. MacQueen. "Some methods for classification and analysis of multivariate observations". In Proc. Fifth Berkeley Symp. Math. Stat. Probab. Vol. 1 Stat., pp. 281–297, Berkeley, Calif., 1967. University of California Press.

[43] A. K. Jain, M. N. Murty and P. J. Flynn. "Data clustering: a review". ACM computing surveys (CSUR), vol.31, no. 3, pp. 264–323, 1999.

[44] T. Kohonen. "Self-organized formation of topologically correct feature maps". Biological Cybernetics, Springer, vol. 43, no. 1, pp. 59–69, 1982.

[45] M. Farooq and A. Hafeez. "Covid-resnet: A deep learning framework for screening of covid19 from radiographs". arXiv preprint arXiv:2003.14395, 2020.

[46] H. S. Maghdid, A. T. Asaad, K. Z. Ghafoor, A. S. Sadiq, S. Mirjalili and M. K. Khan. "Diagnosing COVID-19 pneumonia from X-ray and CT images using deep learning and transfer learning algorithms". In Multimodal image exploitation and learning 2021, volume 11734, p. 117340E. International Society for Optics and Photonics, 2021.

[47] B. King, S. Barve, A. Ford and R. Jha. "Unsupervised Clustering of COVID-19 Chest X-Ray Images with a Self-Organizing Feature Map". Midwest Symposium on Circuits and Systems, vol. 2020-Augus, pp. 395–398, aug 2020.

[48] P. Garg, R. Ranjan, K. Upadhyay, M. Agrawal and D. Deepak. "Multi-scale residual network for covid-19 diagnosis using ct-scans". In ICASSP 2021-2021 IEEE International Conference on Acoustics, Speech and Signal Processing (ICASSP), pp. 8558–8562. IEEE, 2021.

[49] H. Gunraj, L. Wang and A. Wong. "COVIDNet-CT: A Tailored Deep Convolutional Neural Network Design for Detection of COVID-19 Cases from Chest CT Images". Frontiers in Medicine, vol. 7, pp. 1025, 2020.

[50] C. Vogelsanger and C. Federau. "Latent space analysis of vae and intro-vae applied to 3-dimensional mr brain volumes of multiple sclerosis, leukoencephalopathy, and healthy patients". arXiv preprint arXiv:2101.06772, 2021.

[51] A. Wahl, L. E. Gralinski, C. E. Johnson, W. Yao, M. Kovarova, K. H. Dinnon, H. Liu, V. J. Madden, H. M. Krzystek, C. De et al. "SARS-CoV-2 infection is effectively treated and prevented by EIDD-2801". Nature, vol. 591, no. 7850, pp. 451–457, 2021.

[52] P. Angelov and E. Almeida Soares. "SARS-CoV-2 CT-scan dataset: A large dataset of real patients CT scans for SARS-CoV-2 identification". MedRxiv, 2020.

[53] M. Stone. "Cross-validatory choice and assessment of statistical predictions". Journal of the royal statistical society: Series B (Methodological), vol. 36, no. 2, pp. 111–133, 1974.

[54] P. A. Lachenbruch and M. R. Mickey. "Estimation of error rates in discriminant analysis". Technometrics, vol.10, no. 1, pp. 1–11, 1968.

[55] R. Kundu, H. Basak, P. K. Singh, A. Ahmadian, M. Ferrara and R. Sarkar. "Fuzzy rank-based fusion of CNN models using Gompertz function for screening COVID-19 CT-scans". Scientific Reports, vol. 11, no. 1, pp. 1–12, 2021.

[56] S. M. Rezaeijo, M. Ghorvei, R. Abedi-Firouzjah, H. Mojtahedi and H. Entezari Zarch. "Detecting COVID-19 in chest images based on deep transfer learning and machine learning algorithms". Egyptian Journal of Radiology and Nuclear Medicine, vol. 52, no. 1, 2021.

[57] W. Zhao, W. Jiang and X. Qiu. "Deep learning for COVID-19 detection based on CT images". Scientific Reports, vol. 11, no. 1, pp. 1–12, 2021.